Synthesis of _Gallus gallus domesticus_ eggshells and magnetite bio-composite for Cr(VI) removal: adsorption kinetics, equilibrium isotherms and thermodynamics

Huma Ajab[a], Mehpara Khatoon[a], Asim Yaqub[b,*], Muhammad Gulfaraz[c],
Shamyla Nawazish[b], Farhan A. Khan[a], John Ojur Dennis[d], Muhammad Junaid[e]

[a]_Department of Chemistry, COMSATS University Islamabad, Abbottabad Campus, Pakistan, emails: humaajab@cuiatd.edu.pk (H. Ajab); mehparakh@gmail.com (M. Khatoon); farhankhan@cuiatd.edu.pk (F.A. Khan)_
[b]_Department of Environmental Sciences, COMSATS University Islamabad, Abbottabad Campus, Pakistan,_
_emails: environment_green@yahoo.com (A. Yaqub), shamyla@cuiatd.edu.pk (S. Nawazish)_
[c]_University of Arid Agriculture Rawalpindi, Pakistan, email: gulfrazsatti@uaar.edu.pk_
[d]_Universiti Teknologi PETRONAS, Perak Malaysia, email: johndennis@utp.edu.my_
[e]_Department of Information Technology, The University of Haripur, Pakistan, email: mjunaid@uoh.edu.pk_

ABSTRACT

This research study aimed to remove chromium (Cr^{6+}) from aqueous and industrial effluent by natural _Gallus gallus domesticus_ eggshell waste magnetized with Fe_3O_4 nanoparticles (MES). A literature survey showed that the sorption of Cr on the modified magnetite form of this biomass had not been explored before. Structure, morphology, functional groups, and thermal stability of the prepared modified biosorbent were characterized by scanning electron microscopy, X-ray diffraction pattern, Fourier transform infrared spectroscopy, and thermogravimetric analysis. The results of the characterization study confirmed the suitability of Cr adsorption on the proposed adsorbent. The optimization studies were performed to measure the suitable conditions for the adsorption process. The most suitable pH for maximum chromium adsorption by MES was 2. The contact time for maximum adsorption was noted to be 30 min, and the most suitable temperature was found to be 20°C. It was observed that MES showed 95% removal of Cr. The kinetics data for MES followed the pseudo-first-order kinetic model, while the intraparticle diffusion played a significant part in the rate-controlling step. The results described the pseudo-first-order kinetic model for Cr adsorption by MES, with the highest value of correlation coefficient $R^2 = 0.864$. The equilibrium for adsorption data was best described by Langmuir isotherm. For the thermodynamic process, $\Delta G°$, $\Delta H°$, and $\Delta S°$ were calculated, the value of ΔH and ΔS was –34.622 and –0.11 kJ/mol K, respectively, and found that adsorption of Cr was spontaneous and exothermic. The suitability of MES in industrial effluent was also carried out that offers a green, sustainable, cost-effective, and real-world water treatment solution for water purification having Cr from wastewater/industrial effluent.

Keywords: Nanoparticles; _Gallus gallus domesticus_ Eggshells; Biosorption; Chromium

* Corresponding author.

1. Introduction

Hasty industrial expansion is the main reason for heavy metals pollution in an environment, especially in the water bodies worldwide [1]. The heavy metal contamination of aqueous streams is becoming a severe threat to the aquatic ecosystem because of their high toxicity. Heavy metals are not susceptible to biological degradation and usually accumulated in living tissues after entering through the food chain [2]. Cr is considered as one of the top sixteen toxic pollutants because of its carcinogenic characteristics for humans. Oxidation states of Cr such as trivalent and hexavalent are comparatively stable and mostly predominant [3]. These oxidation states influence the Cr toxicity and chemical properties in aqua. Although Cr(III) is less toxic than Cr(VI), but Cr(III) is the reason for structural disorders in erythrocyte membranes [4]. In alkaline media, Cr(III) can quickly oxidize into harmful Cr(IV) due to the presence of strong oxidants in water and soil [5].

Numerous medical studies have verified the ability of Cr(VI) to cause respiratory effects, carcinogenic effects, skin effects, gastrointestinal effects, renal and hepatic effects, haematological effects, cardiovascular effects, genotoxic and mutagenic effects, reproductive and developmental effects [6]. The maximum acceptable level for Cr in drinking water is 0.1 mg/L, which is set by the US EPA [7].

The industries that released Cr into the water are tanneries, battery industry, metallurgical and electroplating industry, steel, agrochemicals, paper and pulp, and fertilizer industries [8]. Numerous techniques are offered to eliminate chromium species from wastewater, such as ion exchange, percolation, chemical precipitation, electro-coagulation, membrane filtration, infiltration and phytoremediation [9]. Amid these approaches, biosorption advantages a special consideration for its comparative ease and low cost [10].

Modified bio sorbents are excellent scavengers among economic adsorbents such as agricultural by-products, waste from industries, ion exchangers' carbons, nano-materials, metal oxides, composites, magnetic nanocomposites, etc. [11]. Among biosorbents, *Gallus gallus domesticus* eggshells (ESs) have been reconnoitered for various practices including polishing or cleansing agent for various surfaces (abrasives) to adsorbents for many metal ions [12]. Studies have been accompanied to conclude the aptness of the ESs as adsorbents for heavy metals and dyes [13]. Marked surveys and breakdowns have been carried out to discover the likelihood of essential applications of ESs, mainly for wastewater. The nature of ESs, that is, porous, creates an eye-catching substance to be recycled as an adsorbent. Each ES is valued for possessing in the range of 7,000 to 17,000 [14]. The chemical composition of *Gallus gallus domesticus* eggshell has been reported as follows: calcium carbonate (94%), organic matter (4%), magnesium carbonate (1%) and calcium phosphate (1%). The eggshell has high surface area and owns an intricate lattice network of even and water-insoluble fibers ensuing in various applications such as adsorbent and immobilization support.

The nano sized materials are now a day's extensively applied for wastewater treatment owing to their high adsorption capacity [15]. Nanocomposites, due to their large surface area and better reactivity, are highly efficient adsorbents, catalysts and sensors. High surface area to-mass ratio of nanocomposites can significantly enhance the adsorption capability [16].

The magnetic nanoparticles have been utilized as components with other adsorbents to help in separation of adsorbents as well as to increase the removal of chromium (Cr) [17]. In this context, the scientists have already used bentonite clay modified with Fe_3O_4 magnetic nanoparticles for the adsorption of Cr [18].

In an aqueous medium, the oxidation of Cr(III) results in more carcinogenic and highly toxic Cr(VI). Trivalent Cr forms hexaaquachromium(III) complex in distilled water. This complex solution is green in color. This complex ion is fairly acidic with a pH range of 2–3. After 24 h, the green color solution changes to violet color complex by the loss of proton from one of the ligand water molecules in aqueous solution and becomes acidic in nature.

The reaction is as follows:

$$[Cr(H_2O)_6]^{3+} \longrightarrow [Cr(H_2O)_5(OH)]^{2+} + H^+ \qquad (1)$$
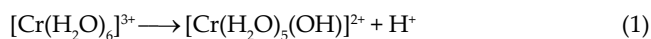
The absorbance of Cr is unstable as in less concentrated solution it is colorless. So in order to overcome this problem, trivalent Cr is converted to hexavalent Cr by oxidation method. This oxidation is carried out by using 1 molar NaOH solution and 3%–4% H_2O_2. By this method, the intense yellow color of hexavalent Cr is obtained. The reaction of Cr with sodium hydroxide and hydrogen peroxide is given as:

$$[Cr(H_2O)_6]^{3+} + 6OH^- \longrightarrow [Cr(OH)_6]^{3-} + 6H^+ \qquad (2)$$

$$[Cr(OH)_6]^{3-} + H_2O_2 \longrightarrow 2CrO_4^{2-} + 2OH^- + 8H_2O \qquad (3)$$
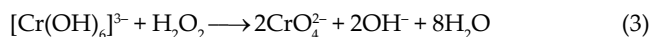
For oxidation of 20 mg/L Cr solution, only 5 mL of 1 molar NaOH solution and 1 drop of H_2O_2 is required [19].

As trivalent Cr is changed to hexavalent Cr so its maximum absorbance was measured spectrophotometrically, which is 374 nm and absorbance of other standard solutions was measured at this wavelength. The present study was designed to remove Cr using modified magnetite-ES biosorbents. These aim to develop more efficient, inexpensive, and eco-friendly adsorbents to remove them initially before being discharged into water bodies. Moreover, the modification of *Gallus gallus domesticus* eggshells with magnetic nanoparticles will also assist in the separation of adsorbents and enhance the removal of Cr from actual world samples. Besides waste management, wastewater remediation and conversion of waste material into the valued product would be an additional benefit by utilizing ES waste to clean the environment. A literature survey showed that the sorption of Cr on the modified magnetite form of this biomass had not been explored before.

In this study, nanoparticle magnetic iron oxide composites of ESs were manufactured and latterly characterized by X-ray diffraction (XRD), scanning electron microscopy (SEM), thermo-gravimetric analysis (TGA), and Fourier transform infrared spectroscopy (FTIR). We also investigate the rate of Cr(VI) adsorption on modified composites and desorption and undergo optimization study concerning pH, temperature, contact time, metal concentration, and adsorbent dose.

The kinetics, equilibrium constants, and thermodynamic parameters were also examined.

2. Materials and methods

Chromium chloride, 3%–4% hydrogen peroxide, iron sulphate ($FeSO_4 \cdot 7H_2O$), hydrochloric acid (HCl), and iron chloride ($FeCl_3 \cdot 6H_2O$) were purchased from Sigma-Aldrich (Germany). The sodium chloride (NaCl) and sodium hydroxide (NaOH) were purchased from DAEJUNG (Korea).

The eggshell waste of *Gallus gallus domesticus* from bakery was gathered from the local market. The washed *Gallus gallus domesticus* eggshells were overnight oven-dried at 20°C. For granulation of *Gallus gallus domesticus* eggshells, a mechanical crusher was used, sieved and then dried in the desiccator. The magnetization of biosorbents was carried out by co-precipitation method [20].

The biosorbents were impregnated with Fe_3O_4 nanoparticles. This modification was carried out by dissolving 3.1 g of $FeCl_3 \cdot 6H_2O$ and 2.1 g of $FeSO_4 \cdot 7H_2O$ in 40 mL of distilled water each. The solutions were then mixed with fast stirring and heating (up to 80°C). pH of the solution was raised by adding 10 mL of NaOH. To this solution, 10 g of eggshell was added and stirred for about 30 min. The solution was then cooled and filtered (Whatman cellulose filters (0.45 μm, 25 mm)). The residue was washed for number of times with distilled water, which was then dried in an oven for 24 h at 102°C. K. Roy's (India) electronic balance was used for weighing purpose.

2.1. Characterization

An X-ray diffractometer (JDX-3532, JEOL) was used to get the X-ray diffraction patterns. SEM (JSM 5910, JEOL Japan) was used to obtain the surface studies of biosorbents. Five kilovolt with different magnification times was applied for the enlargement of the surface. The presence of various functional groups was confirmed with the help of FTIR analysis (PerkinElmer, UK). The thermal stability of the modified eggshell (MES) was conducted through the thermogravimetric analyzer (STA-6000 PerkinElmer, UK).

2.1.1. Point of zero charge

The PZC of magnetically modified biosorbents was found by adding 20 mL of 0.1 mol/dm³ NaCl [21]. The pH was set from 2 to 10 by adding 0.05 M HCl and 0.05 M NaOH, followed by adding 0.1 g of adsorbent (MES) in each flask. After 60 min shaking, the final pH was noted and (ΔpH) was calculated.

2.2. Preparation of Cr solution and batch adsorption test

1,000 mg/L of stock solution of $CrCl_3$ was prepared in deionized water. The calibration curve for Cr was obtained at a wavelength of λ_{max} 374 nm by using a UV-visible spectrophotometer (T80+UV/VIS Spectrometer, PG Instruments Ltd., UK). R^2 value was 0.9943.

The Cr solutions ranging from 5 to 30 mg/L were prepared from 100 mg/L solutions. Each titration flask was filled with 20 mL of each solution. Then 0.1 g of each magnetically modified biosorbent was taken in these flasks followed by 60 min orbital shaking (Mac Mini rotator flask shaker, MSW 303) at room temperature. After 60 min, a magnetic field was applied, and a magnetically modified biosorbent was separated from the solution. The supernatant was collected, and the final concentration of Cr was measured at 374 nm using a UV/visible spectrophotometer. The removal of Cr was calculated in percentage by using Eq. (4):

$$\% \text{ removal} = \frac{C_i - C_e}{C_i} \times 100 \tag{4}$$

where C_e and C_i (mg/L) are the final and initial concentration of Cr at time t (min). These experiments were carried out in triplicate: and the averages were calculated with standard deviation (SD) values.

2.2.1. Effects of MES biosorbent dosage, pH, and temperature

The biosorbent dosage effect was studied from 0.05 to 0.3 g on the metal adsorption on an orbital shaker at room temperature for 60 min. The rate of adsorption was
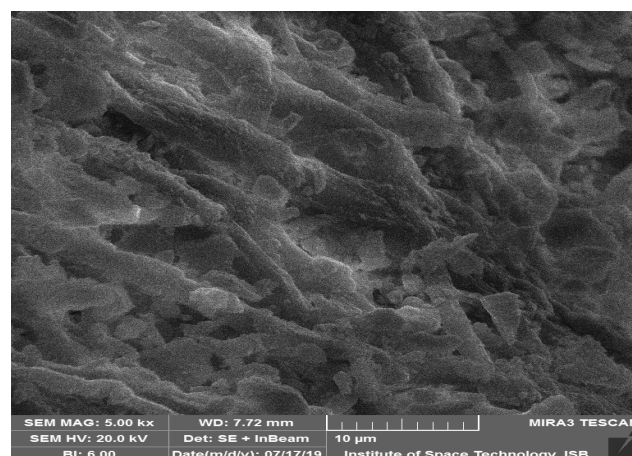
(a)
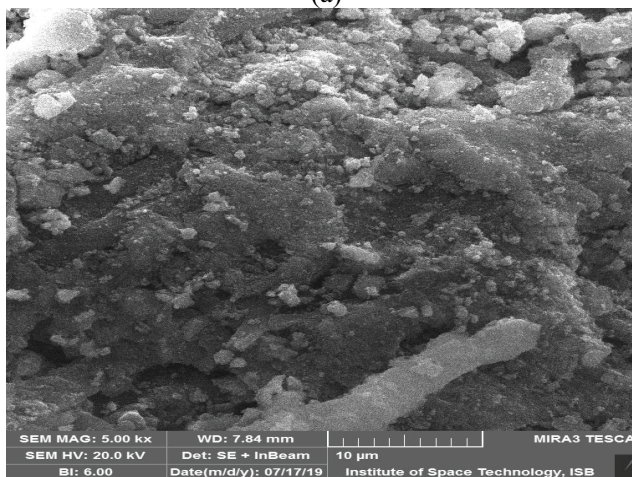
(b)

Fig. 1. SEM images of ES (a) before modification and (b) after modification.

determined concerning changing pH values from 2 to 10 and adjusted 0.05 M HCl and 0.05 M NaOH by a pH meter (Adwa, AD1020, Hungary). The effect of temperature was investigated from 20°C to 60°C adjusted by the water bath (DIAHAN Scientific, Korea) for 30 min.

2.2.2. Kinetic, equilibrium, and thermodynamic studies

From the conditions that were developed in the previous experiments, the thermodynamic, equilibrium, and kinetic studies were established. In the current study, we fitted the adsorption data to different isotherm models such as Langmuir, Temkin, and Freundlich isotherms in order to calculate the data of the process. 5–60 ppm range of solutions was used to study the adsorption of Cr on magnetically MES at room temperature. The kinetics of Cr on MES was determined by measuring the absorbance of Cr after interaction with (0.1 g) of adsorbent at different time intervals, and adsorption at each time was measured using a UV-visible spectrophotometer. The kinetic study data were tested using various kinetic rate models, including pseudo-first-order, pseudo-second-order, and intra-particle diffusion models. The thermodynamic parameters, including the entropy (ΔS (kJ/mol)), free energy (ΔG (kJ/mol)), and changes in enthalpy (ΔH (kJ/mol)), were calculated to describe the adsorption process onto MES.

2.2.3. Batch recovery experiment

0.1 M NaOH and 0.1 M HCl solutions were prepared in distilled water, and we took 50 mL of each solution in different flasks. To these solutions, 30 mg of metal-laden biosorbent (MES) was added. Each of these flasks was shaken at room temperature using an orbital shaker for different time intervals. For each time interval, different recovery equilibrium experiments were carried out. These solutions were digested by 10 mL of 1 M HNO$_3$ solution, and metal ions desorbed were calculated by UV spectrophotometer.

3. Results and discussions

3.1. Adsorbent characteristic

Figs. 1a and b represent ES (before adsorption) and MES (after modification). Before modification, the images showed an irregular, porous pattern and crystalline structure of eggshell particles. This material is spongy with a vast surface having heterogeneous pores, a non-adhesive appearance, and agglomerates. The results are in strong agreement with the study by Tizo et al. [22]. The porous and abundant layering structures with cavities of the eggshell are indeed responsible for its good adsorbing capacity [23]. After reinforcement with Fe$_3$O$_4$ MNPs (modified nanoparticles), the porous structure reflects a narrow size distribution of nanoparticles. The crosslink between ES and Fe$_3$O$_4$ results in the change in morphology and, for that reason increasing the vacant sorption sites and assisting the adsorption aptitudes of Cr. Because of Fe$_3$O$_4$NPs even coating, the protein fibers of underneath membrane eggshell were adequately covered, which results in providing an even and stable platform for the adsorption of Cr [24].

Fig. 2 shows the crystalline phases of the MES, which were identified with XRD. The diffraction peaks were compared with Joint Committee on Powder Diffraction Standards (JCPDS) and International Center for Diffraction Data (ICDD-PDF-2) database to explore the phases of preliminary and adsorbed materials. It was observed that the nature of the material is crystalline. In Fig. 2, the peak intensity confirms the incorporation of nanoparticles. The characteristic diffraction peaks at 2θ = 29.45°, 33.9°, 36.9°, 48.43°, and 57.62°, corresponded with the planes at (220), (311), (222), (440), and (511), respectively, which is in strong accordance with Fe$_3$O$_4$ nano-particles (Reference code 00-001-11111). Based on XRD analysis, one can describe the formation of composite by Fe$_3$O$_4$ and biosorbents.

Fig. 3 shows the bending and stretching vibrations of the functional groups on MES responsible for the adsorption of the Cr molecules. Similarly, the spectral characteristic of both original and loaded biomass, that is, MES before and after adsorption, are presented in Table 1. The bands shifting and the fluctuations in the intensity of signal sanction the identification of the functional groups responsible for metal sorption. Different chemical groups such as carbonates, hydroxyl, carbonyl, carbonates, etc. have been recognized for the biosorption of heavy metals. Strong peaks at 1,417 and 1,411 cm^{-1} in unloaded and loaded biomass can be strictly related to the existence of carbonate minerals inside the matrix of the eggshell. Two peaks at 710 and 871 cm^{-1} (Fig. 3a), 670 and 865 cm^{-1} (Fig. 3b) were also observed, which are allied by means of in- and out-plane distortion, correspondingly signifying the existence of calcium carbonate (CaCO$_3$). The purposes of the eggshell as an adsorbent possibly will interact with Cr in an aqueous solution since the spectrum of carbonate groups are present. The peak observed at 3,415 and 3,339 cm^{-1} must be assigned to the occurrence of an alcohol hydroxyl group. The bands at 2,929 and 2,532 cm^{-1} signify C–H vibrations, representing the existence of the organic layers, fabricated from amino acids present in the *Gallus gallus domesticus* eggshells. Bands at 1,631 and 1,611 cm^{-1} assign to (C=O) carbonyl group stretching and amide,
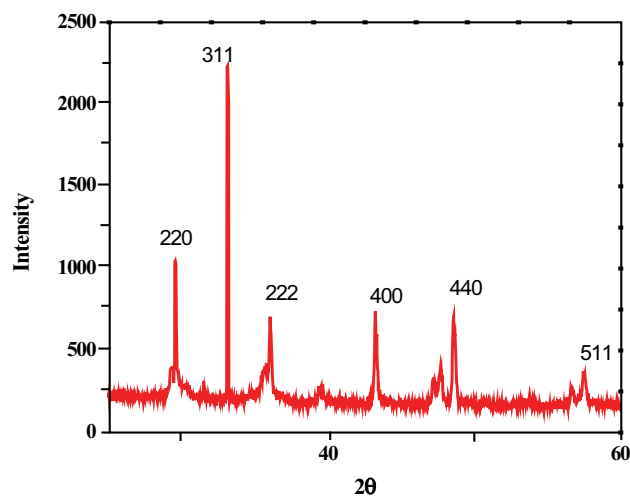
Fig. 2. X-ray diffraction of MES.
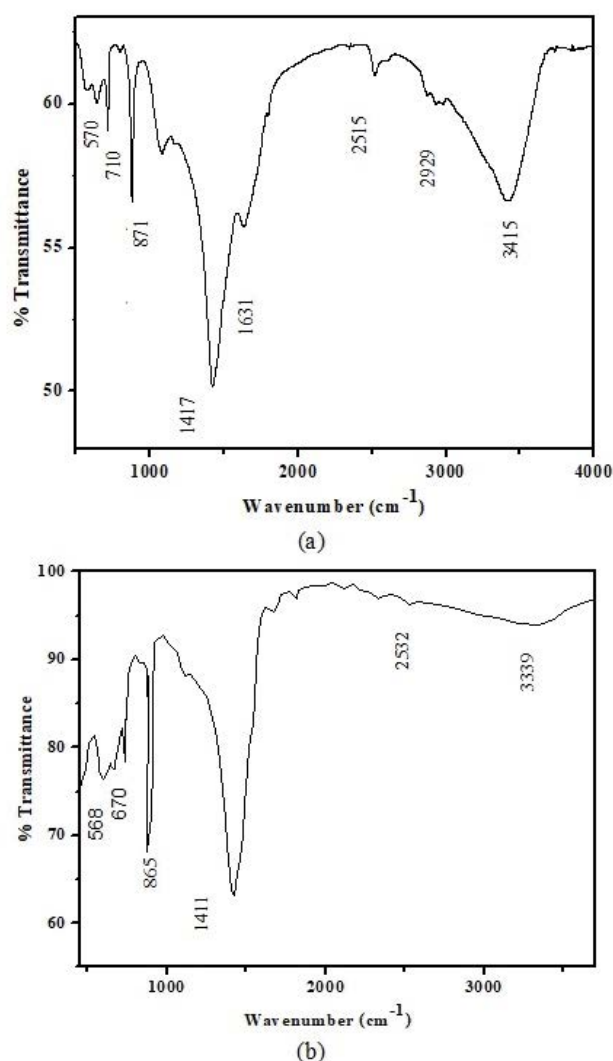
Fig. 3. Fourier transform infrared spectroscopy spectrum of MES before Cr adsorption (a) and MES after Cr adsorption (b).

respectively [25]. The decrease in peak intensity and peak frequency confirmed the adsorption of Cr by MES. Furthermore, the Fe–O peak at 570 and 568 cm⁻¹ confirmed the incorporation of Fe_3O_4 on biosorbents [26]. Whereas in comparison of the original biomass and with the biomass

residue of Cr-loaded, the shifting of some functional group peaks en route for the low energy level was observed. Metallic ion confers to have organic functional groups, increase the bond length and decrease of electron density due to the attraction of the negatively charged electrons cloud from the functional group, so that the absorption peaks which are present in the Cr-loaded biomass residue scrutinized to the lesser energy level [27]. From the FTIR spectra results, it is confirmed that the proposed adsorbent has the features to be utilized as potential biosorbent.

Thermo-gravimetric analysis (TGA) is practiced to measure the weight/mass change and the rate of weight change as a function of temperature, time, and atmosphere [28]. The measurements are practiced mainly to find the composition and thermal stability of materials. The weight loss of MES at a temperature range from 0°C to 700°C is revealed in Fig. 4. That can be observed the loss of weight reduced gradually from 0°C to 200°C and declined rapidly from 200°C to 600°C. The weight loss in the temperature range of 100°C to 600°C is owed to slight disintegration of the organic material proteins into small molecules such as CO_2, CO (commencing from organic fraction), and H_2O molecules [29]. While a significant weight loss in the temperature range of 600°C–700°C is due to the loss of carbon dioxide from the carbonate present in *Gallus gallus domesticus* eggshells [30]. The decrease in the weight of the material was noted after heating it to 700°C with an increasing temperature of 5°C/min.

3.2. Adsorption of Cr on MES

3.2.1. Point of zero charge

The PZC value defines the condition when the density of an electrical charge present on the adsorbent surface equal to zero [31]. It describes the type of adsorbate and adsorbent interface. The surface of the adsorbent is positively charged, which attracts the anions below the PZC while at above PZC, the surface is negatively charged, which attracts cations [32]. The PZC plot (Fig. 5) shows that the point of zero value of eggshell approximately falls at pH 8.

3.2.2. Effect of pH

In adsorption studies, the pH is a significant factor because it is involved in metal speciation and protonation of binding sites of metals [33] and therefore intensely affects

Table 1
Fourier transform infrared spectroscopy frequency analysis of magnetized eggshells of *Gallus gallus domesticus* before and after the absorption of chromium

Frequency before adsorption (cm⁻¹)	Frequency after adsorption (cm⁻¹)	Possible functional group
3,415	3,339	Hydroxyl group stretching
2,929	2,532	C–H bending vibration
1,417	1,411	Carbonate groups of stretching
570	568	Fe–O bond
1,631	1,611	Carbonyl group stretching
710–871	670–865	C–H bending vibration
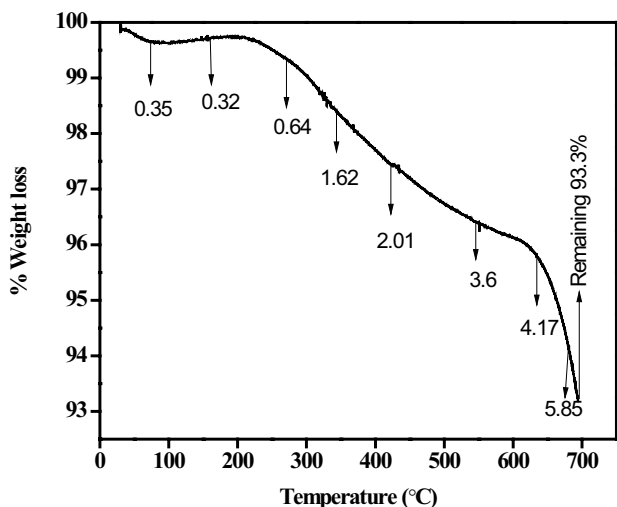
Fig. 4. TGA analysis of MES.
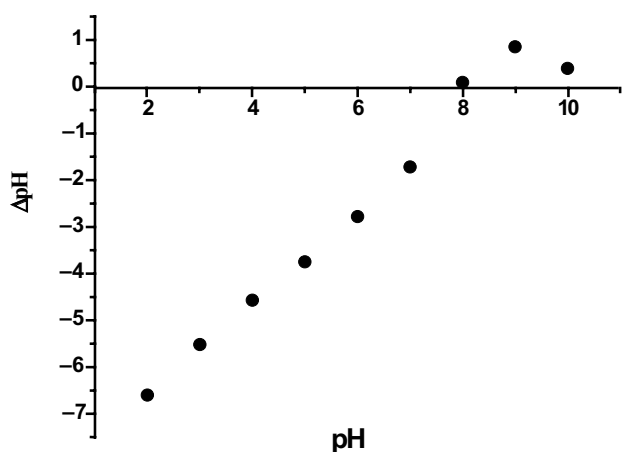
Fig. 5. Point of zero charge plot of MES.

the adsorption rate of various metals on the surface of biosorbents in an aqueous medium. It has been found from the literature that at pH below 2, Cr(III) is the predominant species while $Cr(OH)_3$ is the predominant specie between pH 6.5 and 10 [34]. While at pH 4, the Cr(III) and $Cr(OH)^{2+}$ species are existing nearly 40% and 60% dissemination, respectively. At pH 5, the $Cr(OH)^{2+}$ species present 70% of the Cr with 20% other forms as $Cr_3(OH)_4^{5+}$. At pH 6, $Cr(OH)^{2+}$ and $Cr_3(OH)_4^{5+}$ species signify 40%, 35%, and 25% approximate of the aqueous Cr. The effect of pH on the rate of Cr adsorption by modified biosorbent was studied, as shown in Fig. 6a. The results showed that the maximum adsorption of Cr by ES was at pH 2, which is about 86%. Adsorption of Cr by MES may involve the electrostatic interaction, hydrogen bonding, and ion exchange mechanism [35].

The effect of pH is described by PZC value of modified ES. Cr metal in solution exists in the form of negatively charged ions such as $Cr_2O_7^{2-}$, $HCrO_4^-$, and CrO_4^{2-} [36]. Thus, the more percentage removal will be at pH below PZC. Another study also reported that functional groups become negatively charged as the pH increases. When

pH is below 4, Fe^{2+} existed mainly in the form of ion, and when pH is above 4, Fe^{2+} existed as Fe(OH) and $Fe(OH)_2$ [37]. At pH below PZC, the surface of the adsorbent became positively charged due to the formation of $Fe-OH^{2+}$ [38]. So, the Cr anions adsorption occurred, and hereafter, the pH study showed that the percentage removal of Cr at acidic pH was significantly high. So, acidic pH favored the maximum adsorption of Cr, and the rate of adsorption decreases towards alkaline pH.

3.2.3. Effect of MES biosorbent dosage

Adsorption of Cr dramatically depends upon the dose of adsorbent. The results showed that the percentage removal of Cr enhances with the increase in adsorbent dose up to 75%, but on further increase in adsorbent dosage, the decrease in adsorption rate was observed. The results of the effect of adsorbent dosage have been displayed in Fig. 6b.

Dose-dependent adsorption of Cr different amounts of biosorbent (0.05–0.3 g) was studied. It was found that initially, the Cr removal for modified MES increased up to 0.25 g of adsorbent dose because of the presence of a large number of adsorption sites, and then a decrease in adsorption rate was observed due to overlapping of adsorption sites.

3.2.4. Effect of initial concentration of Cr

The initial metal ion concentration influences the metal uptake process significantly in aqueous solutions. The particular sites in the biosorbents adsorb the metal ions. These specific sites get saturated with increasing metal ion concentration. Equilibrium adsorption data at different concentrations of metal ions in solutions are necessary to establish the efficiency of an adsorbent. Different concentrations of Cr were selected, ranging from 5 to 60 ppm, to determine the efficiency of modified adsorbents for the Cr metal removal from wastewater. For MES, up to a certain point, the increase in adsorption with the increase in metal concentration was observed, and then a decrease in percentage removal was measured. The increase in percentage removal is due to the faster diffusion rate of Cr on active pores of modified ES but the reason for the decrease in adsorption rate could be that a finite number of adsorption sites are present for a given mass of adsorbent [39]. These sites became saturated up to certain metal ion concentrations; thus, adding more metal concentration cannot increase the adsorption rate as all sites were occupied [40]. The adsorption of Cr on magnetically modified ES was studied at room temperature. The solutions used were in the range of 5–60 ppm. Fig. 6c shows that the rate of adsorption of Cr first increased and then decreased when the concentration of the solution was increased. Fig. 7 shows the effect of contact time and initial Cr concentration on adsorption capacity (q_e).

3.2.4.1. Equilibrium study

The adsorption process is described by different isotherms. Adsorption isotherms are the plots that represent the interaction among adsorbents and adsorbate. The sorption
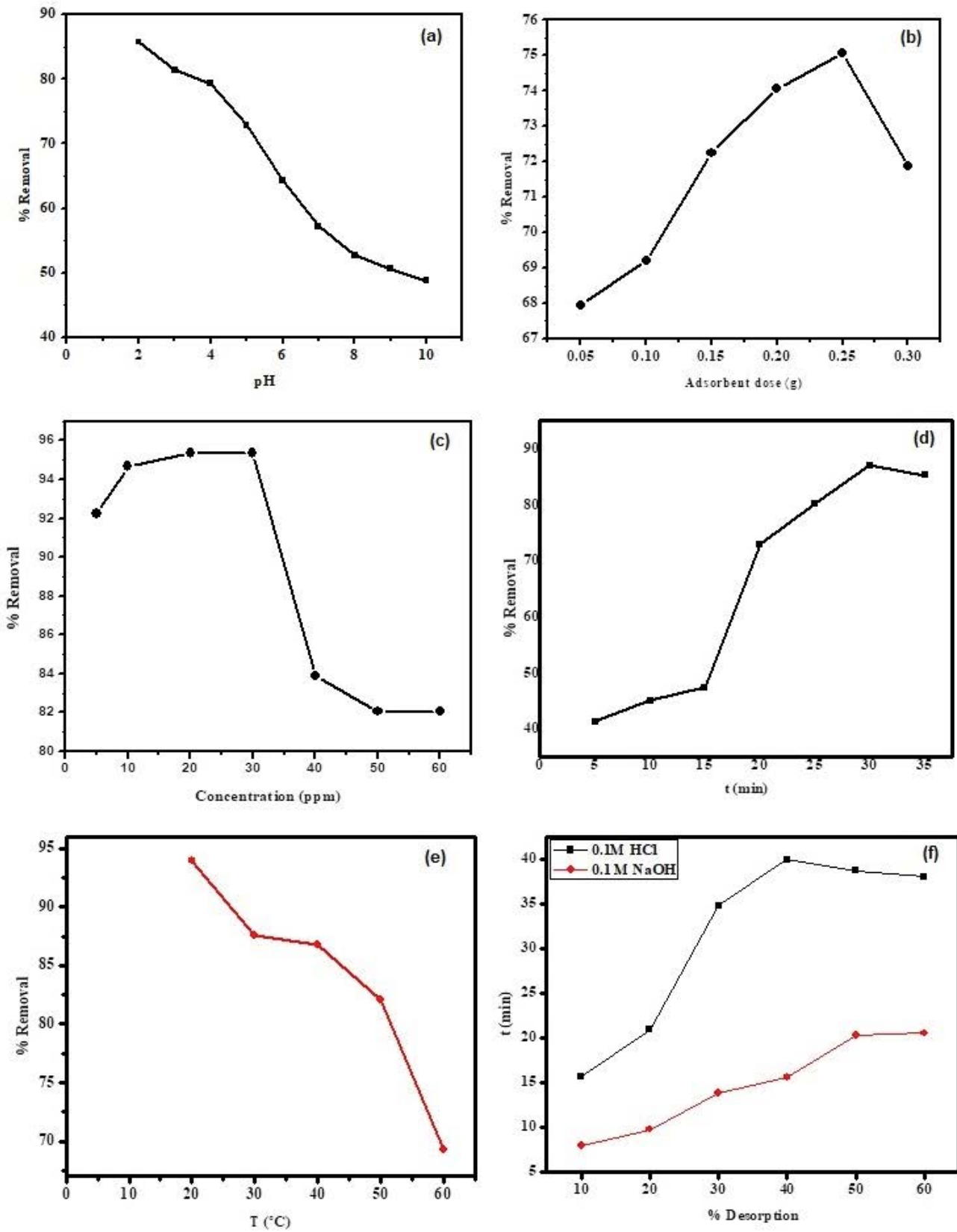
Fig. 6. Effect of pH (a), adsorbent dose (b), concentration (c), time (d), temperature, (e) on adsorption of Cr on MES and desorption study (f).
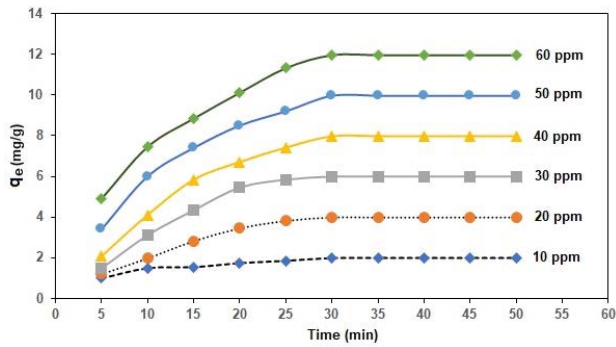
Fig. 7. Effect of time and initial Cr concentration on adsorption capacity (q_e) by ES.

capacity of an adsorption catalyst depends on the concentration of pollutants. The sharper and steeper rise of the isotherm indicates the more effective adsorption capacity [41]. The adsorption data fitted to different isotherm models (Langmuir, Freundlich, and Temkin isotherms) as shown in Figs. 8a–c. The values of isotherm constants besides R^2 values are given in Table 2. The linear form of Langmuir and Freundlich and Temkin isotherm models are presented in Eqs. (5)–(7), respectively.

$$\frac{1}{q_e} = \left(\frac{1}{q_m K_L}\right)\frac{1}{C_e} + \frac{1}{q_m} \tag{5}$$

$$\ln q_e = \ln K_f + \frac{1}{n}\ln C_e \tag{6}$$

$$q_e = B \ln K_t + B \ln C_e \tag{7}$$

where K_f = adsorption capacity, n = heterogeneity factor, K_t = equilibrium binding constant, B = heat of adsorption, q_e = amount of adsorbate adsorbed per unit mass of adsorbent, C_e = equilibrium concentration, q_m = maximum monolayer adsorption capacity.

According to the present study, the linearity was achieved for all three models, but the Langmuir model showed very good fitting in terms of regression coefficient (R^2 = 0.947). Therefore, in contrast to tested models (Table 2) for the description of Cr(VI) adsorption equilibrium isotherms on MES is as follows: Langmuir > Temkin > Freundlich. This indicated homogenous distribution of active sites on MES biosorbent and the formation of Cr monolayer in these sites. The Langmuir model evaluates the maximum adsorption capacity build on the assumption of a homogeneous and monolayer exposure of adsorbate onto an indistinguishable set of well-defined confined biosorption sites starved of lateral interface and steric interruption among biosorbed molecules [42].

3.2.5. Effect of contact time

The effect of contact time on sorption can be evaluated for the possible rapidness of binding, and metal ions
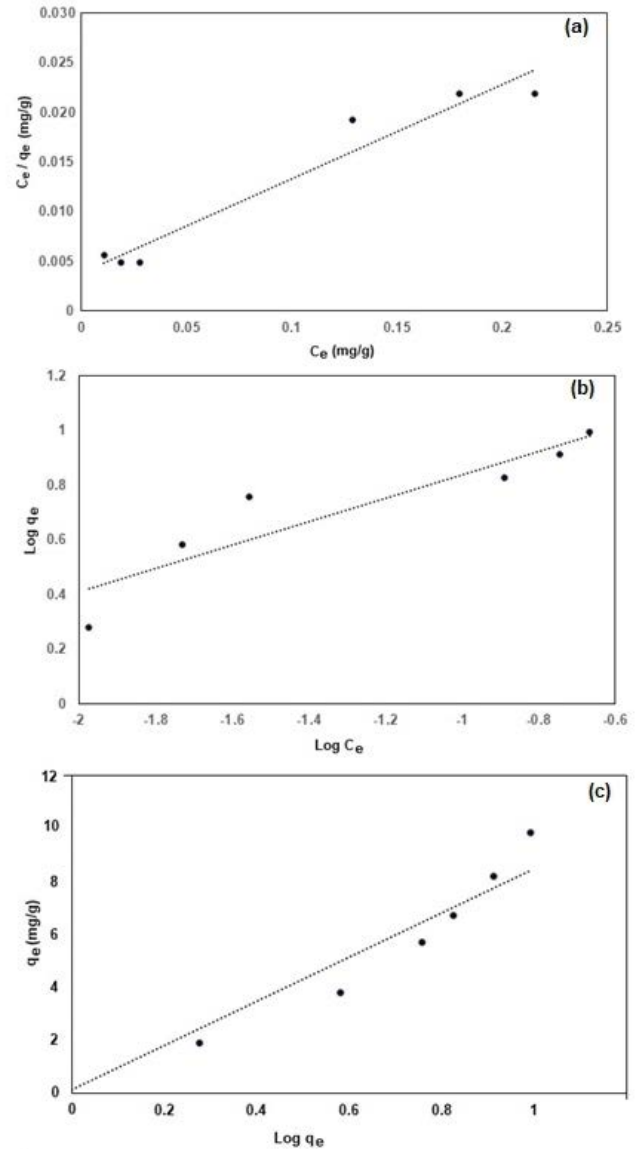
Fig. 8. Linear Langmuir (a) Freundlich, (b) and Temkin (c) plot for Cr adsorption on MES.

Table 2
Different adsorption isotherm of Cr using magnetized eggshells of *Gallus gallus domesticus*

Models	Parameters	Value
Langmuir adsorption isotherm	q_m (mg/g)	10.54
	K_L (L/mg)	0.041
	R^2	0.947
Freundlich adsorption isotherm	K_F (mg/g)	18.35
	R^2	0.843
	n	2.37
Temkin adsorption isotherm	K_T	1.02
	R^2	0.911
	B	8.37

removal by the adsorbent. The sorption contact time of Cr on modified ES is shown in Fig. 6d. The quick and rapid sorption rate for the initial period is principally based on the availability of active sites on the biosorbent surface responsible for facilitating the accumulation of Cr ions on the eggshell. For ES, the metal uptake was continuously increasing with time from 40% to 90%. At first, the solute concentration was high as all the adsorbent sites were vacant, which results in an increased rate of metal uptake. Finally, the adsorption equilibrium stage was approached, wherever the adsorption and desorption rates were found equal, and no further apparent rise in percentage removal was noticed. The percentage removal with time indicated the transfer of ions of metal from the liquid phase to the adsorbent surface.

3.2.5.1. Kinetic study

The biosorption kinetic is one of the most imperative properties while describing the rate and mechanism of biosorption and able to be used to aid design suitable biosorption technologies. It is appropriate for any designated biosorption system to reveal high sorption capacity and fast sorption rate [43]. The kinetic study data fitted to different kinetic rate equations such as pseudo-first-order, pseudo-second-order, and intra-particle diffusion model and the following equations represent these models:

$$\log(q_e - q_t) = \log q_e - \left(\frac{k_1}{2.303}\right)t \tag{8}$$

$$\frac{t}{q_t} = \frac{1}{k_2 q_e^2} + \left(\frac{1}{q_e}\right)t \tag{9}$$

Adsorption capacity q_e (mg/g) is at equilibrium and adsorption capacity is q_t at time t (min), K_1 (min^{-1}), and K_2 (g/mg min) are rate constants of pseudo-first-order and pseudo-second-order kinetics correspondingly. Figs. 9a–c and Table 3 encapsulate the values of kinetic coefficients achieved for these kinetic models along with regression coefficients (R^2). It was found that the pseudo-first-order model is more suitable for the description of the kinetic behavior of adsorption with the highest value of $R^2 = 0.864$ (correlation coefficient), showing that the reaction rate was adsorbate and adsorbent dependent. The pseudo-second-order has lower values of R^2 and, therefore, is not suitable to explain the kinetics of Cr adsorption on MES. The adsorption capacity at equilibrium (q_e) value calculated from slopes and intercepts of graph plotted was in good agreement by experimental (q_e) value in case of pseudo-first-order model.

The Weber and Morris plot, which is also known as intra-particle pore diffusion, is also commonly used to describe the sorption data. According to this model, the rate-limiting step is the one in which diffusion of adsorbate takes place inside the pores of adsorbent particle, that is, intraparticle diffusion, a plot of q_t against $t^{1/2}$ should be a straight line using slope k_i and intercept C when adsorption mechanism follows the intra-particle diffusion process [44]. The parameters of the intra-particle diffusion model in the
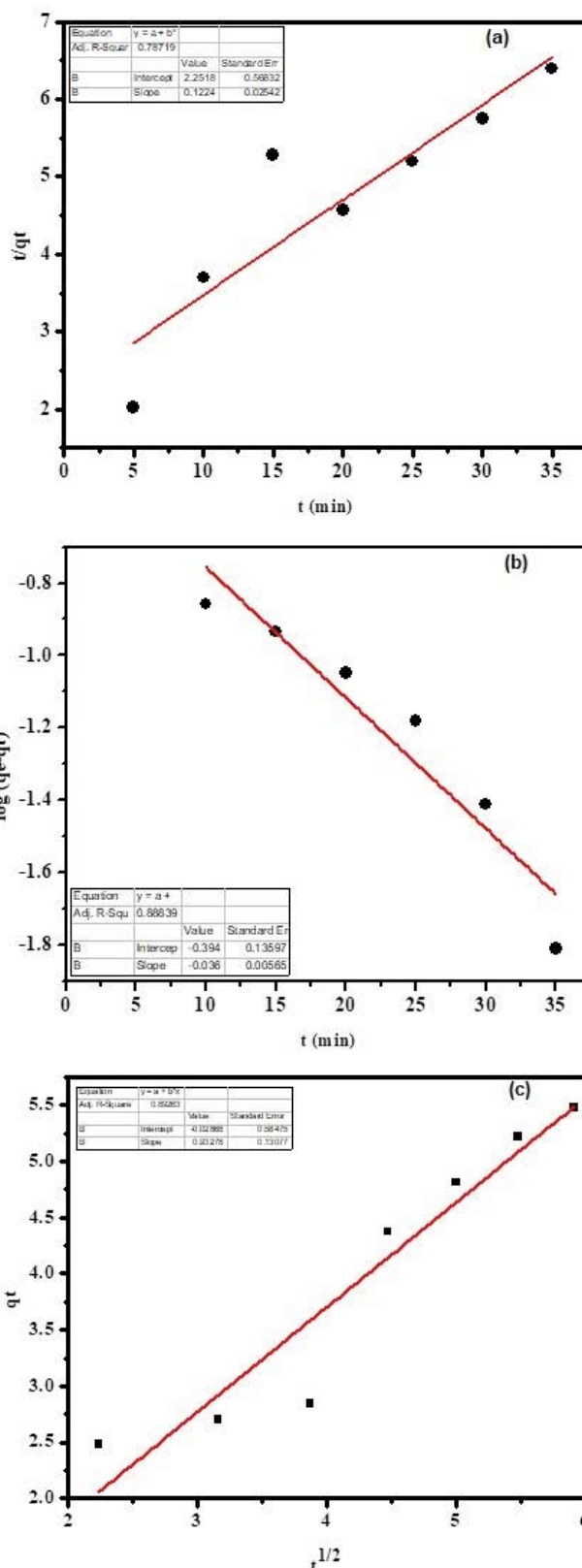
Fig. 9. Pseudo-second order model (a) pseudo-first-order model (b) and intraparticle diffusion model (c) of Cr adsorption on MES.

Table 3
Kinetics parameters of Cr using magnetized eggshells of *Gallus gallus domesticus*

Models	Parameters	Value
Pseudo-second-order kinetic model	q_e (mg/g)	8.169
	k_2	0.0066
	R^2	0.787
Pseudo-first-order kinetic model	K_1 (min^{-1})	–0.09
	q_e (mg/g)	7.24
	R^2	0.864
Intra-particle diffusion model	K_{int}	0.976
	R^2	0.892
	I	0.413

present study showed relatively good interaction and diffusion rate in the adsorption system, and the equation is given as follows:

$$q_t = k_p t^{1/2} + C \tag{10}$$

where k_p = diffusion rate constant; C = intercept of the linearity plot.

3.2.6. Effect of temperature

Temperature plays a vital role in optimizing the adsorption process as it impacts the rate of adsorption by varying the solubility potential and adsorbate molecular interactions. TThe influence of the temperature by MES was examined with the was examined with the initial Cr concentration of 30 ppm using the range of temperature from 20°C to 60°C. For MES, the results showed that an increase in temperature negatively influenced the decrease in percentage removal, representing exothermic adsorption. It was due to increased solubility of calcium carbonate at elevated temperature as ES are composed of calcium carbonate. The skeleton of ES is made up of organic matter and carbonates. The calcium ions concentration is bound through ion exchange and therefore can be replaced by other cations, which are Cr ions in this case. Thus at higher a temperature, the solubility of Cr increases and decrease biosorption capacity of ES [45]. The increase in temperature and the decrease in adsorption capacity might be owed to the breaking of internal bonds or due to weakening force among the active sites of the adsorbent and Cr. These results are a reasonable covenant with that reported by Alkan et al. [46]. The effect of temperature with percentage removal is given in Fig. 6e.

3.2.6.1. Thermodynamic study

To examine the spontaneity and thermodynamic feasibility of adsorption of Cr on MES, different parameters of thermodynamic such as enthalpy change (ΔH), Gibbs free energy change (ΔG) and entropy change (ΔS) were determined using the following thermodynamic equations.

$$\Delta G = \Delta H - T\Delta S \tag{11}$$

$$\ln K_d = \frac{\Delta S}{R} - \frac{\Delta H}{RT} \tag{12}$$

where K is the adsorption equilibrium constant, and R is the general gas constant. Slope and intercept of the plot of $\ln K_d$ vs. $1/T$ were computed for enthalpy, and entropy changes as shown in Fig. 10 and Table 4 showing the value of ΔH, ΔS and ΔG. The values of ΔG were negative, increasing with temperature verified the spontaneity of adsorption process, and it reveals the positive influence of temperature on adsorption of Cr on Fe_3O_4-nanoparticles, which is identical with the exothermic nature of the process of adsorption [47].

The value of ΔH was also negative, which specifies the exothermic nature of the process, and accordingly, the absorption of energy while breaking the bond is lower as compared with the energy released in the formation of bonds and thus liberating energy in the form of heat. While the negative value of ΔS exposes the decline of the randomness of the solid–liquid interface, by no significant variations in the inside structure of the adsorbents via adsorption process [48]. Parallel performance of getting negative values for thermodynamic parameters was noticed by Miraboutalebi et al. [49].

3.3. Desorption study

The desorption study of Cr on MES was performed by using 0.1 M NaOH and 0.1 M NaOH as shown in Fig. 6f. The highest desorption from the metal-laden MES was detected in acidic medium. As in an acidic medium, the metal ions were replaced by protons, and the functional groups of the biosorbents became protonated. Thus the release of metal ions from biosorbents occurred. While in basic medium, less desorption was observed due to deprotonating, hence metal ions find it hard to be separated from the surface of the biosorbents.
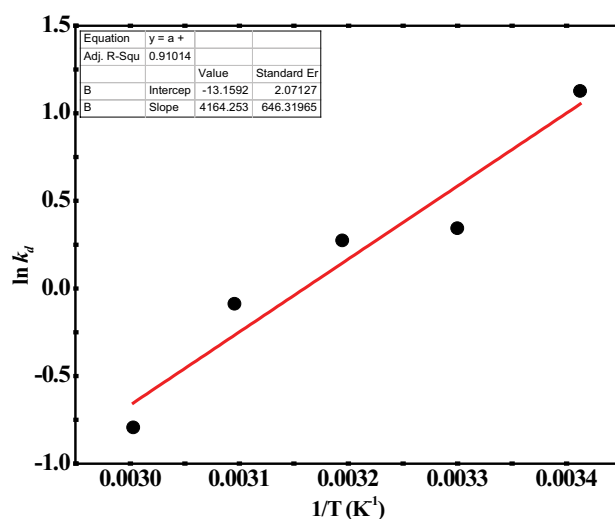
Fig. 10. Plot of $\ln K_d$ vs. $1/T$ for Cr adsorption on MES.

Table 4
Thermodynamic parameters of Cr adsorption on magnetized eggshells of *Gallus gallus domesticus*

Temperature (K)	ΔG (kJ/mol)	ΔH (kJ/mol)	ΔS (kJ/mol)
293	–2.567		
303	–1.473		
313	–0.379	–34.622	–0.11
323	0.715		
333	1.808		

3.4. Comparison study of MES with other adsorbents for Cr removal

Upon comparison of MES with other eggshell biomass-based adsorbents for Cr removal, it was confirmed that the adsorption capacity of our MES is good enough in comparison with others results reported by different researchers, as set in Table 5. The present research study elucidated that the magnetically modified ES is a better and environmental friendly adsorbent for wastewater treatment. This high % removal of MES is attributed to the porous nature and presence of a higher concentration of $CaCO_3$ on ES coupled with large a surface area of magnetite nanoparticles that is strongly supported by desorption study, making it a better and environmental friendly adsorbent for wastewater treatment. Here it is valuable to say that the most commonly used activated carbon as an adsorbent is known for its effective removal due to its structural characteristics. Still, the problem is the same, it is not economically favorable and difficult to regenerate. Thus alternatively, locally available, eco-friendly and low-cost adsorbent such as MES could be better a alternative that can be further removed or separated from medium.

3.5. Application of MES for Cr removal from the effluent of leather tanning industry

On a laboratory scale, the removal of Cr by MES was very successful. For the actual sample application, the effluent from the leather tanning industry was collected. After removing suspended solids, the initial Cr concentration present in the effluent was 20 mg/L found by spectrophotometer. Then under optimum conditions, filtrate was treated with magnetically modified ES and the final concentration of Cr was measured with spectrophotometer.

Table 5
Comparison table

Adsorbents	Amount of Cr removal	Reference
Eggshells	49%	[47]
Eggshells	48.1%	[48]
Eggshells membrane	81.4%	[49]
Eggshells	25%	[6]
Eggshells	30%	[50]
Eggshell	59.46%	[51]
MES	95%	[Present study]

The results indicated that 72% Cr (5.6 ± 0.6 mg/L) was removed from the absolute sample. The overall study concluded that the magnetically modified ES to be a suitable adsorbent to adsorb Cr from wastewater.

3.6. Proposed mechanism of adsorption by Gallus gallus domesticus, magnetized eggshells

The proposed mechanism can be illustrated by using SEM analysis for predicting modification, and the FTIR and PZC analysis as a confirmation of the electrostatic interaction, and ion exchange mechanism for the adsorption of Cr anions.

SEM and XRD images of the biosorbents shows porous surface for supporting the incorporation of Fe_3O_4 nano-particles, which results in the magnetic modification of biosorbents to enhance Cr adsorption.

Chromium metal in solution exists in the form of negatively charged ions such as $Cr_2O_7^{2-}$, $HCrO_4^-$, and CrO_4^{2-}, so an electrostatic interaction will occur between negatively charged Cr ions and the positively charged magnetized adsorbent. At pH below PZC, the surface of the adsorbent became positively charged due to the formation of $Fe-(OH)_2^+$. So, chromium anions adsorption occurred as a result of electrostatic interaction.

The ion exchange equipment here will be porous magnetized *Gallus gallus domesticus* eggshells (which acts as a micro-porous exchange resin) supersaturated with Cr ions. The $Fe-(OH)_2^+$ will act as charged beads on the surface of the proposed MES resin. As water passes through this resin bed, the Cr ion will attach to the MES resin beads releasing the solution from the toxic Cr ions. The exchange resins, that is, MES, are regenerated by stirring with a salt brine solution.

The electrostatic confirmation for the adsorption of Cr anions can be illustrated by band analysis of FTIR and the value of PZC. While the ion exchange mechanism is a subject to further studies.

The band of CO_3^{2-} is observed at the wavenumbers of 712, 875 and 1,427 cm^{-1} that are common to $CaCO_3$. The absorption bands due to stretching of water molecules are observed around 3,400–3,600 cm^{-1}. The C–H stretching bands are observed at about 3,000–2,400 cm^{-1}. The decrease in peak intensity and peak frequency confirmed the adsorption of Cr by magnetized adsorbents. Furthermore, the Fe–O peak at 570 cm^{-1} confirmed the incorporation of Fe_3O_4 on biosorbents.

The attraction of anions and cations occurs at the pH below and above the PZC value, respectively. The PZC value obtained for ES was at pH 8. The effect of pH on rate of Cr adsorption by modified biosorbents was studied, and the results showed that the maximum adsorption of Cr by ES occurred at pH 2, which depicts the adsorption of anions.

4. Conclusions

The surface-modified biomass was found to be worthy for the adsorption of Cr from the solution. The adsorption capacity of MES (q_e (mg/g)) was noted to be 12 mg/g. The point of zero charge was found to be 8, indicating that the functional groups became positively charged below this

pH, which favored anionic adsorption. The effect of different parameters on Cr uptake was studied, and it was found that the adsorption was increasing with increasing Cr concentration, time, and amount of adsorbents. The maximum adsorption was observed at pH 2 for MES. Upon characterization study, the MES revealed important characteristics such as porosity, functional groups, surface charge, and thermal stability, which can optimize the adsorption capacity. The feasibility of the process was confirmed by Langmuir model of isotherm. The kinetic data of the adsorption system for MES were best described by the pseudo-first-order model. The thermodynamic parameters such as ΔG and ΔH confirmed that the adsorption was feasible, spontaneous, and exothermic. At the same time, ΔS recommends a reduction on the disorder on the interface solid/solution through the adsorption of Cr on MES. This research exhibits the effective conversion of agricultural waste into a valuable biosorbent to apply Cr from wastewater/industrial effluent.

References

[1] G. Yaylalı-Abanuz, Heavy metal contamination of surface soil around Gebze industrial area, Turkey Microchem. J., 99 (2011) 82–92.

[2] M. Arora, B. Kiran, S. Rani, A. Rani, B. Kaur, N. Mittal, Heavy metal accumulation in vegetables irrigated with water from different sources, Food Chem., 111 (2008) 811–815.

[3] J. Guertin, Toxicity and Health Effects of Chromium (All Oxidation States), Chromium(VI) Handbook, CRC Press, USA, 2004, pp. 215–234.

[4] H.P. Singh, P. Mahajan, S. Kaur, D.R. Batish, R.K. Kohli, Chromium toxicity and tolerance in plants, Environ. Chem. Lett., 11 (2013) 229–254.

[5] J. Hu, C. Chen, X. Zhu, X. Wang, Removal of chromium from aqueous solution by using oxidized multiwalled carbon nanotubes, J. Hazard. Mater., 162 (2009) 1542–1550.

[6] M.S. Sankhla, M. Kumari, M. Nandan, R. Kumar, P. Agrawal, Heavy metals contamination in water and their hazardous effect on human health-a review, Int. J. Curr. Microbiol. Appl. Sci., 5 (2016) 759–766.

[7] World Health Organization, Chromium in Drinking-water (No. WHO/HEP/ECH/WSH/2020.3), World Health Organization, Geneva, 2020.

[8] S. Elabbas, L. Mandi, F. Berrekhis, M.N. Pons, J.P. Leclerc, N. Ouazzani, Removal of Cr(III) from chrome tanning wastewater by adsorption using two natural carbonaceous materials: eggshell and powdered marble, J. Environ. Manage., 166 (2016) 589–595.

[9] S. Elabbas, N. Adjeroud, L. Mandi, F. Berrekhis, M.N. Pons, J.P. Leclerc, N. Ouazzani, Eggshell adsorption process coupled with electrocoagulation for improvement of chromium removal from tanning wastewater, Int. J. Environ. Anal. Chem., (2020) 1–13.

[10] A. Hansda, V. Kumar, A comparative review towards potential of microbial cells for heavy metal removal with emphasis on biosorption and bioaccumulation, World J. Microbiol. Biotechnol., 32 (2016) 1–14.

[11] Q. Huang, S. Song, Z. Chen, B. Hu, J. Chen, X. Wang, Biochar-based materials and their applications in removal of organic contaminants from wastewater: state-of-the-art review, Biochar, 1 (2019) 45–73.

[12] T.C. Jeremias, T. Pineda-Vásquez, F.R. Lapolli, M.Á. Lobo-Recio, Use of eggshell as a low-cost biomaterial for coal mine-impacted water (MIW) remediation: characterization and statistical determination of the treatment conditions, Water Air Soil Pollut., 231 (2020) 1–17.

[13] J. Mohammadnezhad, F. Khodabakhshi-Soreshjani, H. Bakhshi, Preparation and evaluation of chitosan-coated eggshell

[14] A. Mittal, M. Teotia, R.K. Soni, J. Mittal, Applications of egg shell and egg shell membrane as adsorbents: a review, J. Mol. Liq., 223 (2016) 376–387.

[15] I. Gehrke, A. Geiser, A. Somborn-Schulz, Innovations in nanotechnology for water treatment, Nanotechnol. Sci. Appl., 8 (2015) 1–17.

[16] G. Sharma, A. Kumar, S. Sharma, H. Ala'a, M. Naushad, A.A. Ghfar, F.J. Stadler, Fabrication and characterization of novel Fe⁰@guar gum-crosslinked-soya lecithin nanocomposite hydrogel for photocatalytic degradation of methyl violet dye, Sep. Purif. Technol., 211 (2019) 895–908.

[17] F.L. Rivera, F.J. Palomares, P. Herrasti, E. Mazario, Improvement in heavy metal removal from wastewater using an external magnetic inductor, Nanomaterials, 9 (2019) 1508.

[18] H.M. Harbi, A.H. Al-Baqawi, M.S. El-Shahawi, Clay minerals functionalized by magnetite (Fe₃O₄) nanoparticles as solid platform for removal of chromium(VI) from water: characterization, kinetics, thermodynamics, analytical utility and reusability studies, Anal. Chem. Lett., 10 (2020) 636–653.

[19] D. Lakherwal, Adsorption of heavy metals: a review, Int. J. Environ. Res. Dev., 4 (2014) 41–48.

[20] M. Kamranifar, A. Naghizadeh, F. Masoudi, F. Osmani, M. Davoodi, M.R. Nabavian, Nitrate removal from aqueous solutions by cobalt ferrite nanoparticles synthesized by co-precipitation method: isotherm, kinetic and thermodynamic studies, Water Sci. Technol., 82 (2020) 2250–2258.

[21] M. Nasiruddin Khan, A. Sarwar, Determination of points of zero charge of natural and treated adsorbents, Surf. Rev. Lett., 14 (2007) 461–469.

[22] M.S. Tizo, L.A.V. Blanco, A.C.Q. Cagas, B.R.B.D. Cruz, J.C. Encoy, J.V. Gunting, R.O. Arazo, V.I.F. Mabayo, Efficiency of calcium carbonate from eggshells as an adsorbent for cadmium removal in aqueous solution, Sustainable Environ. Res., 28 (2018) 326–332.

[23] R. Bhaumik, N.K. Mondal, B. Das, P. Roy, K.C. Pal, C. Das, A. Baneerjee, Eggshell powder as an adsorbent for removal of fluoride from aqueous solution: equilibrium, kinetic and thermodynamic studies, E. J. Chem., 9 (2012) 1457–1480.

[24] Z. Sarikhani, M. Manoochehri, Removal of toxic Cr(VI) ions from water sample a novel magnetic graphene oxide nanocomposite, Int. J. New. Chem., 7 (2020) 30–46.

[25] M. Naghizadeh, M.A. Taher, L.Z. Nejad, F.H. Moghaddam, Fabrication, characterization and theoretical investigation of novel Fe₃O₄@egg-shell membrane as a green nanosorbent for simultaneous preconcentration of Cu(II) and Tl(I) prior to ETAAS determination, Environ. Nanotechnol. Monit. Manage., 10 (2018) 171–178.

[26] M. Shamsipur, L. Farzin, M.A. Tabrizi, S. Sheibani, Functionalized Fe₃O₄/graphene oxide nanocomposites with hairpin aptamers for the separation and preconcentration of trace Pb²⁺ from biological samples prior to determination by ICP MS, Mater. Sci. Eng., C, 77 (2017) 459–469.

[27] A.S.K. Kumar, N. Rajesh, Exploring the interesting interaction between graphene oxide, Aliquat-336 (a room temperature ionic liquid) and chromium(VI) for wastewater treatment, RSC Adv., 3 (2013) 2697–2709.

[28] N. Babanejad, A. Farhadian, I. Omrani, M.R. Nabid, Design, characterization and in vitro evaluation of novel amphiphilic block sunflower oil-based polyol nanocarrier as a potential delivery system: raloxifene-hydrochloride as a model, Mater. Sci. Eng., C., 78 (2017) 59–68.

[29] B. Engin, H. Demirtaş, M. Eken, Temperature effects on egg shells investigated by XRD, IR and ESR techniques, Radiat. Phys. Chem., 75 (2006) 268–277.

[30] W. Praikaew, W. Kiatkittipong, K. Kiatkittipong, N. Laosiripojana, N. Viriya-empikul, S. Boonyasuwat, S. Assabumrungrat, Synthesis of glycerol carbonate from dimethyl carbonate and glycerol using CaO derived from eggshells, MATEC Web Conf., 192 (2018) 03045.

[31] A.N. Frumkin, O.A. Petrii, B.B. Damaskin, Potentials of Zero Charge, In: Comprehensive Treatise of Electrochemistry, Springer, Boston, MA, 1980, pp. 221–289.

[32] C. Jung, J. Heo, J. Han, N. Her, S.J. Lee, J. Oh, Y. Yoon, Hexavalent chromium removal by various adsorbents: powdered activated carbon, chitosan, and single/multi-walled carbon nanotubes, Sep. Purif. Technol., 106 (2013) 63–71.

[33] D.S. Smith, R.A. Bell, J.R. Kramer, Metal speciation in natural waters with emphasis on reduced sulfur groups as strong metal binding sites, Comp. Biochem. Physiol. C: Toxicol. Pharmacol., 133 (2002) 65–74.

[34] G.R.R. Bernardo, R.M.J. Rene, Chromium(III) uptake by agro-waste biosorbents: chemical characterization, sorption–desorption studies, and mechanism, J. Hazard. Mater., 170 (2009) 845–854.

[35] S. Wang, M. Wei, Y. Huang, Biosorption of multifold toxic heavy metal ions from aqueous water onto food residue eggshell membrane functionalized with ammonium thioglycolate, J. Agric. Food Chem., 61 (2013) 4988–4996.

[36] Q. Wang, T. Feng, S. Xiong, Preparation of GO-based iron-containing and adsorption of Cr in water, IOP Conf. Ser.: Mater. Sci. Eng., 472 (2019) 012085.

[37] Y. Cui, M. Liu, H. Huang, D. Zhang, J. Chen, L. Mao, Y. Wei, A novel one-step strategy for preparation of Fe_3O_4-loaded Ti_3C_2 MXenes with high efficiency for removal organic dyes, Ceram. Int., 46 (2020) 11593–11601.

[38] S. Rajput, C.U. Pittman Jr., D. Mohan, Magnetic magnetite (Fe_3O_4) nanoparticle synthesis and applications for lead (Pb^{2+}) and chromium (Cr^{6+}) removal from water, J. Colloid Interface Sci., 468 (2016) 334–346.

[39] J. Ooi, L.Y. Lee, B.Y.Z. Hiew, S. Thangalazhy-Gopakumar, S.S. Lim, S. Gan, Assessment of fish scales waste as a low cost and eco-friendly adsorbent for removal of an azo dye: equilibrium, kinetic and thermodynamic studies, Bioresour. Technol., 245 (2017) 656–664.

[40] M.A. Al-Ghouti, N.R. Salih, Application of eggshell wastes for boron remediation from water, J. Mol. Liq., 256 (2018) 599–610.

[41] A. Saravanan, P.S. Kumar, C.F. Carolin, S. Sivanesan, Enhanced adsorption capacity of biomass through ultrasonication for the removal of toxic cadmium ions from aquatic system: temperature influence on isotherms and kinetics, J. Hazard. Toxic Radioact. Waste, 21 (2017) 04017004.

[42] N. Azouaou, Z. Sadaoui, A. Djaafri, H. Mokaddem, Adsorption of cadmium from aqueous solution onto untreated coffee grounds: equilibrium, kinetics and thermodynamics, J. Hazard. Mater., 184 (2010) 126–134.

[43] O. Abdelwahab, Y.O. Fouad, N.K. Amin, H. Mandor, Kinetic and thermodynamic aspects of cadmium adsorption onto raw and activated guava (*Psidium guajava*) leaves, Environ. Prog. Sustainable Energy, 34 (2015) 351–358.

[44] A.H. Jawad, R.A. Rashid, R.M. Mahmuod, M.A.M. Ishak, N.N. Kasim, K. Ismail, Adsorption of methylene blue onto coconut (*Cocos nucifera*) leaf: optimization, isotherm and kinetic studies, Desal. Water Treat., 57 (2016) 8839–8853.

[45] M.A. Zulfikar, H. Setiyanto, Adsorption of congo red from aqueous solution using powdered eggshell, Int. J Chem. Technol. Res., 5 (2013) 1532–1540.

[46] M. Alkan, Ö. Demirbaş, M. Doğan, Adsorption kinetics and thermodynamics of an anionic dye onto sepiolite, Microporous Mesoporous Mater., 101 (2007) 388–396.

[47] H. Çiftçi, B. Ersoy, A. Evcin, Synthesis, characterization and Cr(VI) adsorption properties of modified magnetite nanoparticles, Acta Phys. Pol. A, 132 (2017) 564–569.

[48] G. Arslan, I. Sargin, M. Kaya, Hexavalent chromium removal by magnetic particle-loaded micro-sized chitinous egg shells isolated from ephippia of water flea, Int. J. Biol. Macromol., 129 (2019) 23–30.

[49] S.M. Miraboutalebi, S.K. Nikouzad, M. Peydayesh, N. Allahgholi, L. Vafajoo, G. McKay, Methylene blue adsorption via maize silk powder: kinetic, equilibrium, thermodynamic studies and residual error analysis, Process Saf. Environ., 106 (2017) 191–202.